

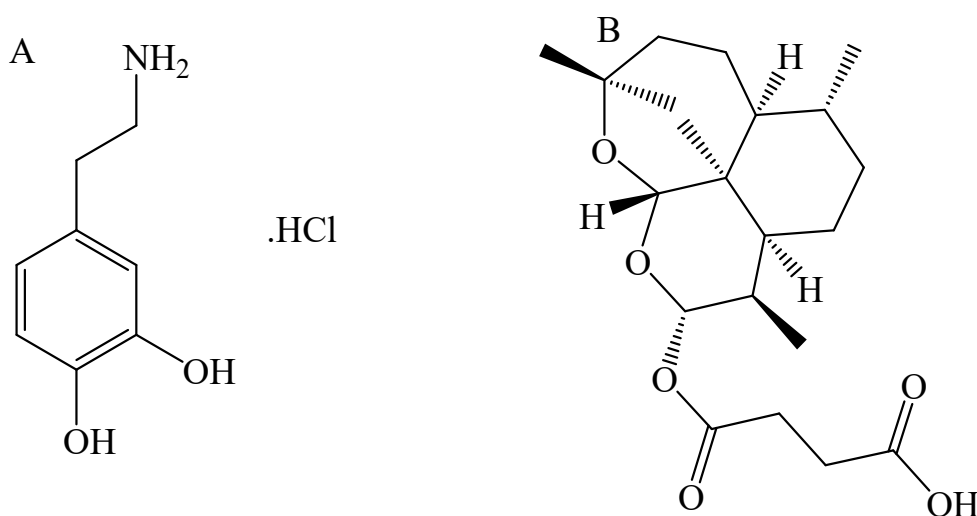
# Synthesis and validation of ultrasensitive stripping voltammetric sensor based on polypyrrole@ZnO/Fe<sub>3</sub>O<sub>4</sub> core-shell nanostructure for picomolar detection of artesunate and dopamine drugs

Mona Elfiky <sup>a\*</sup>, Mohamed Gaber <sup>a</sup>, Maie Mousa, Nehal Salahuddin <sup>a\*</sup>

<sup>a</sup> Chemistry Department, Faculty of Science, Tanta, 31527, Egypt.

Tel.: +201004155414; fax: +91 1332 273560

E-mail address: [Elfiky\\_mona@science.tanta.edu.eg](mailto:Elfiky_mona@science.tanta.edu.eg) & [nehal.ataf@science.tanta.edu.eg](mailto:nehal.ataf@science.tanta.edu.eg)



**Scheme. S<sub>1</sub>:** (A) Structure of Dopamine (DA), and (B) Artesunate (ART)

## 2.1. Materials and instrumentation

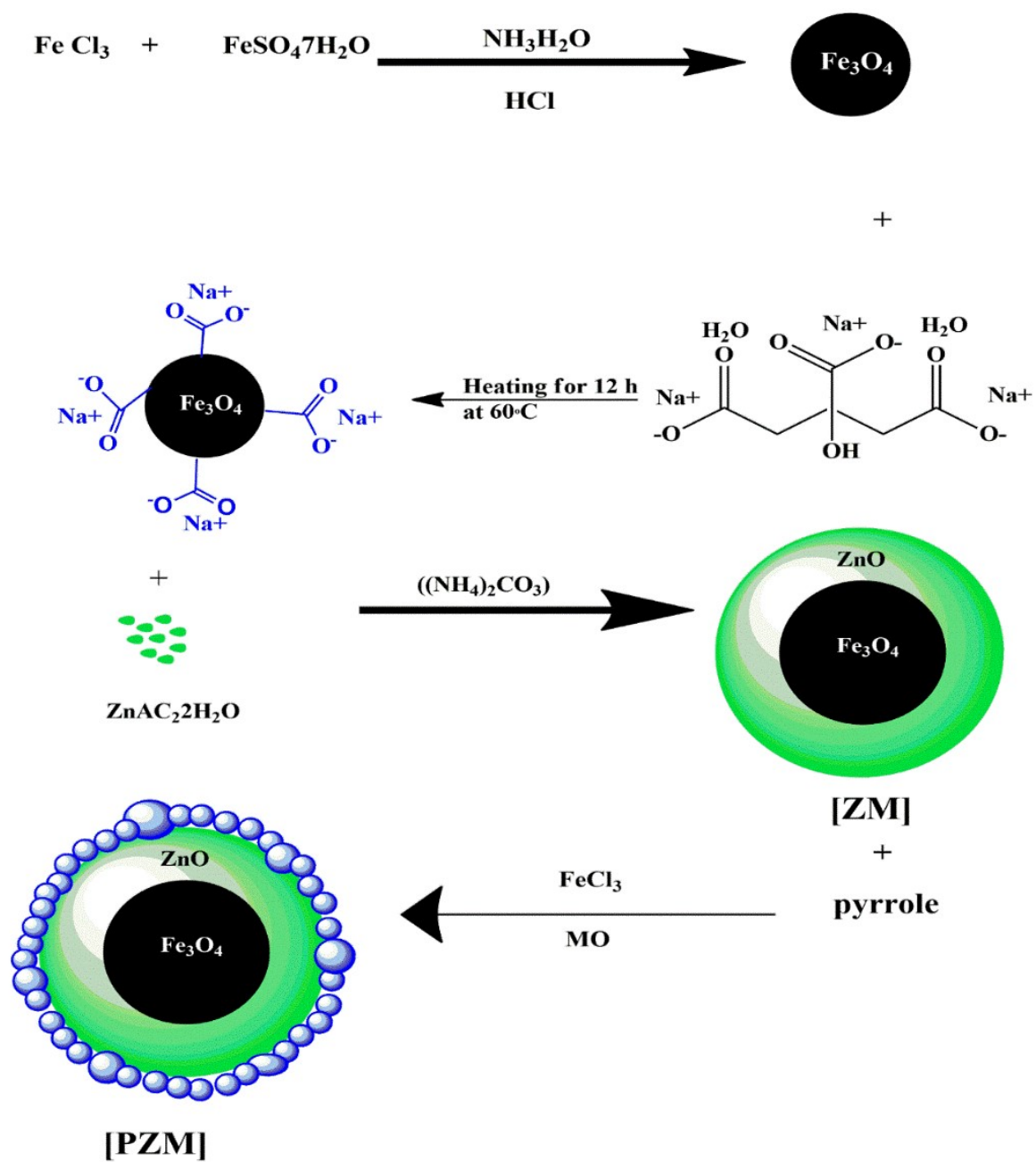
Pyrrole (Ppy, Mallinckrodt, USA, reagent grade, 98%) purified by passing through a column of alumina neutral, sodium citrate (Across, USA,  $\geq 98.0\%$ ), acetic acid (HAc, Alfa Aesar, AR, 99.7%), phosphoric acid (H<sub>3</sub>PO<sub>3</sub>, 99.0%), boric acid (H<sub>3</sub>BO<sub>3</sub>, 99.5%), ammonium carbonate (NH<sub>4</sub>)<sub>2</sub>CO<sub>3</sub>, and glacial acetic acid (CH<sub>3</sub>COOH, 99.0%) were all purchased from Sigma Aldrich. Anhydrous ferric chloride (FeCl<sub>3</sub>, Alpha Chemika, India Reagent grade, 97%), ferrous sulfate (FeSO<sub>4</sub>·7H<sub>2</sub>O, Oxford Lab Chem, India SISCO, 98%), methyl orange (MO, Pubchem), sodium

hydroxide (NaOH pellets, 98.0%) and hydrochloric acid (HCl, 35%) (Adwic, Egypt), zinc acetate dihydrate ( $\text{Zn}(\text{CH}_3\text{COO})_2 \cdot 2\text{H}_2\text{O}$ , MERCK, Darmstadt), artesunate (ART;  $\text{C}_{19}\text{H}_{28}\text{O}_8$ , 384.421 g/mol, China), and dopamine HCl (DA, Sigma Aldrich) were purchased and used as received.

The nature of the interaction between functional groups of as-prepared materials in the wave-number range from 400–4000  $\text{cm}^{-1}$  using potassium bromide disc was determined using a Fourier transform infrared spectroscopy (FTIR) instrument (Shimadzu FTIR-8101 A). To characterize the crystalline nature of all as-prepared samples, an X-ray diffractometer (XRD, Philips PW 1710) equipped with Cu-K $\alpha$  radiation ( $\lambda = 1.54060 \text{ \AA}$ ), voltage (40 kV), and current (30 mA) was used with scanning speed of 0.02°/min and  $2\theta$  with a range from 2 to 80°. Magnetic hysteresis (M-H) curves of some of the as-prepared materials were measured in a magnetic field in the range of –8 and 8 KOe at room temperature. By adding drops of dispersed materials in a mixture of ethanol and DDW, a high-resolution transmission electron microscopy (HR-TEM) instrument (JEM2100 JEOL) is used to investigate the morphological structure and particle size of [ZM], and [PZM]. The surface morphology of [ZM], and [PZM] was also investigated using scanning electron microscopy (SEM) (SU8000 2.0 kV 4.0 mm  $\times$  25.0 K SE (U) equipped with energy-dispersive X-ray spectroscopy (EDX) at an operating voltage of 10 kV. Dynamic light scattering was used to determine the size distribution of the nanoparticle (dynamic light scattering (DLS); Zetasizer Nano ZS; Malvern Instruments, Malvern, UK).

Electrochemical impedance of as-prepared samples was recorded using computer-controlled PAR (Princeton Applied Research, Oak Ridge, TN, USA) potentiostat models Versa STAT 4 using frequency range of 0.1 to 10000 Hz. Voltammetric measurements were performed using computer-controlled electrochemical analyzer models 263A and 394-PAR (Princeton Applied Research, Oak Ridge, TN, USA) with the software package 270/250-PAR. We used a sensor assembly (303A-

PAR) that included a micro-electrochemical cell and a three-sensor system that included a CP as the working sensor, Ag/AgCl/KCl as the reference electrode, and platinum wire as the auxiliary electrode was used. DP-AdCV scans with all as-prepared sensors were tested utilizing a conventional 10-mL volume electrolysis cell containing specific concentration of ART, and DA drug solution mixed with 5 mL of DDW, and then filled with 5 mL of supporting electrolyte (B–R buffer series) under selected preconcentration parameters. DP-AdCV scans were then evaluated after a standing a specific preconcentration time in the selected negative potential range. After each data point was estimated, five-time repetitions were measured in a fresh buffer solution, to refresh the surface of the sensor, under the same potential scan range. The pH drift method <sup>1</sup> has been used to evaluate the pH point of zero charge ( $\text{pH}_{\text{ZPC}}$ ) of **[PZM]**. Briefly, different samples of 20 mL 0.01 M  $\text{NaNO}_3$  solutions was adjusted ( $\text{pH}_i$ ) in the range of 2.0–10 by adding 0.1 M  $\text{HNO}_3$  or  $\text{NaOH}$ . Then, 0.06 g of **[PZM]** was inserted to each sample of  $\text{NaNO}_3$  solution with continuous stirring for 48 h. The pH of the filtrate solution was recorded ( $\text{pH}_f$ ). Then, the  $\text{pH}_{\text{ZPC}}$  of the **[PZM]** was evaluated from the plot of  $\delta\text{pH}$  ( $\text{pH}_f - \text{pH}_i$ ) vs.  $\text{pH}_i$ .



Scheme. S<sub>2</sub>: Synthesis of [ZM], and [PZM].

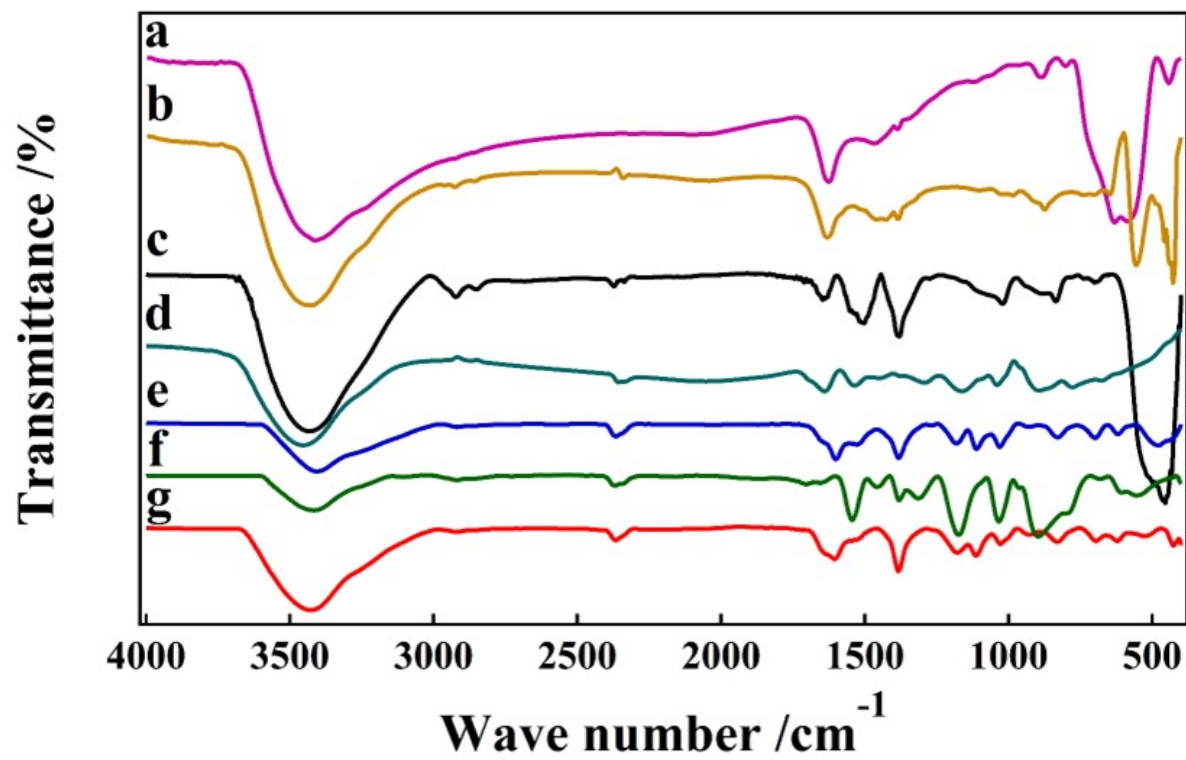


**Figure. S<sub>1</sub>:** FTIR spectra of (a) Fe<sub>3</sub>O<sub>4</sub> NPs, (b) ZnO NPs, (c) [ZM], (d) Ppy, (e) [PZ], (f) [PM], and (g) [PZM].

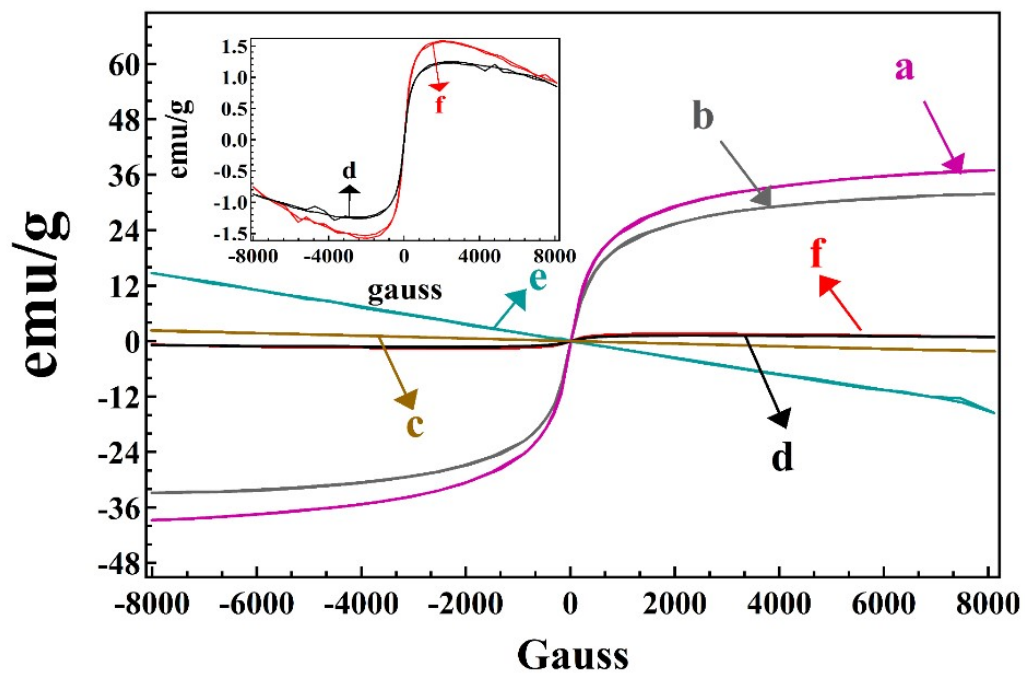


**Figure. S<sub>2</sub>:** Magnetization vs. applied magnetic field at room temperature (a) ZnO NPs, (b) Fe<sub>3</sub>O<sub>4</sub> NPs, (c) Cs@Fe<sub>3</sub>O<sub>4</sub> NPs, (d) [ZM], (e) Ppy, and (f) [PZM].

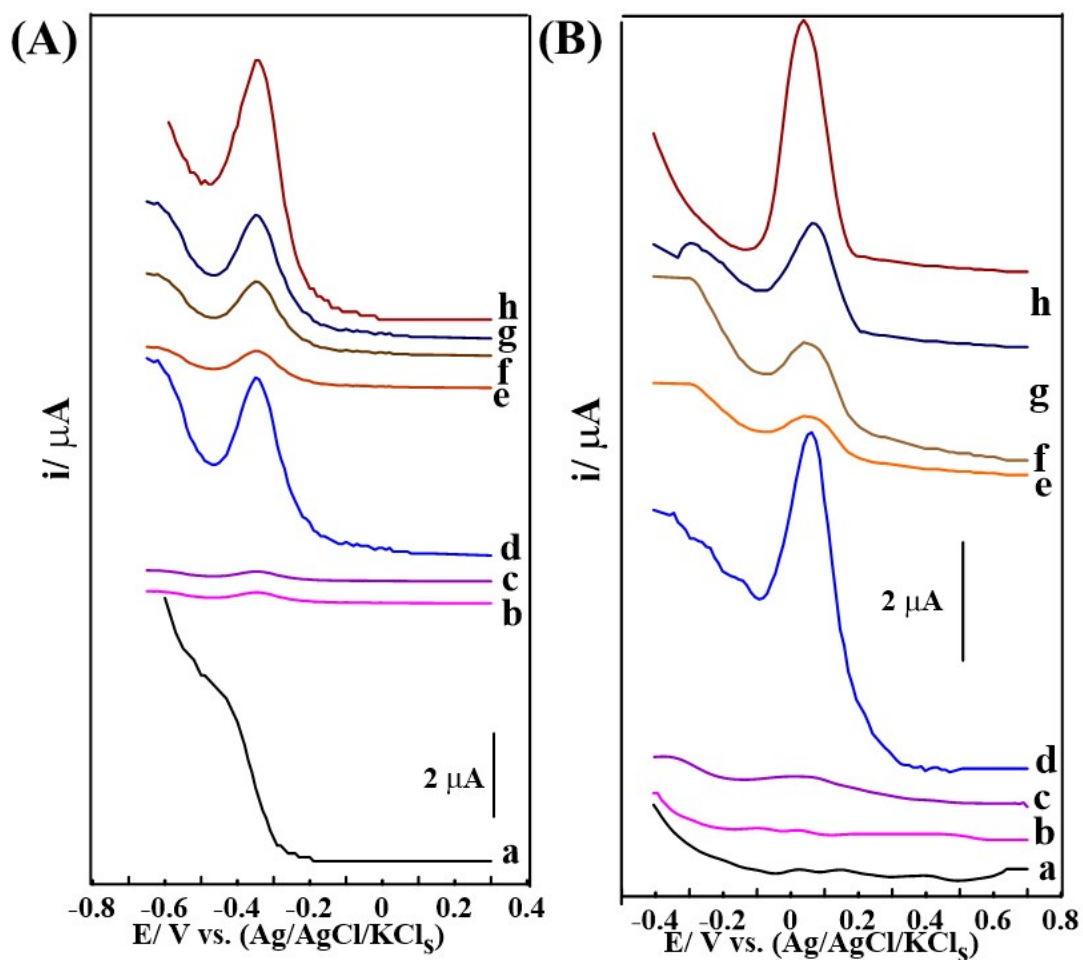


**Figure. S3:** DP-AdCV crests of (A) 10.0 pM of ART in the BR buffer pH 10, and (B) 20.0 pM DA in the BR buffer pH 2 for 70s using (a) BCPS, (b) ZnO NPs, (c) Sc@Fe<sub>3</sub>O<sub>4</sub> NPs, (d) [ZM], (e) Ppy, (f) [PZ], (g) [PM], and (h) [PZM] MCPSs ( $\nu = 120$  mV, and  $\alpha = 45$  mV).

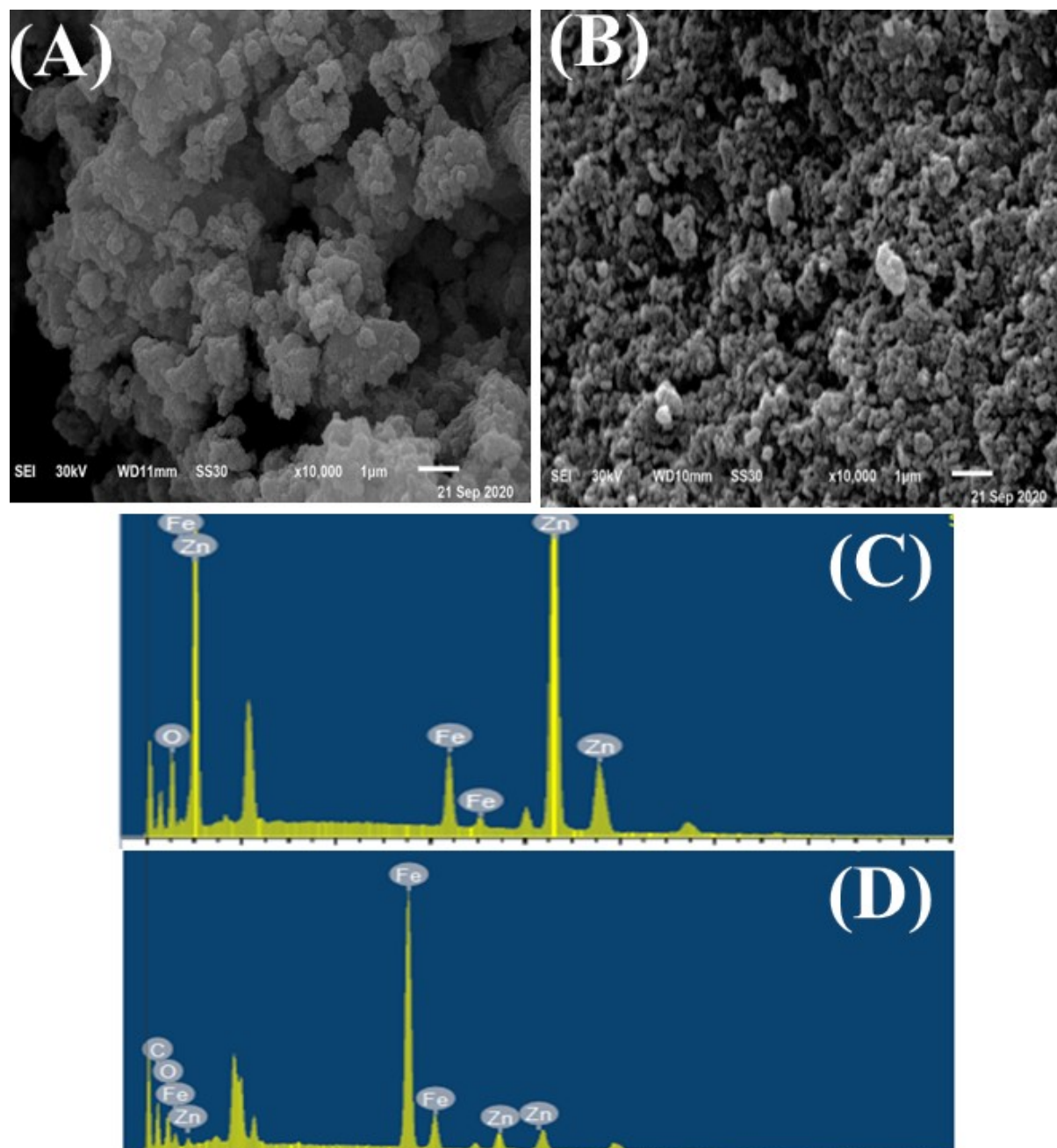


**Figure. S<sub>4</sub>:** SEM images of (A) [ZM], and (B) [PZM]. The EDX analysis of (C) [ZM], and (D) [PZM].



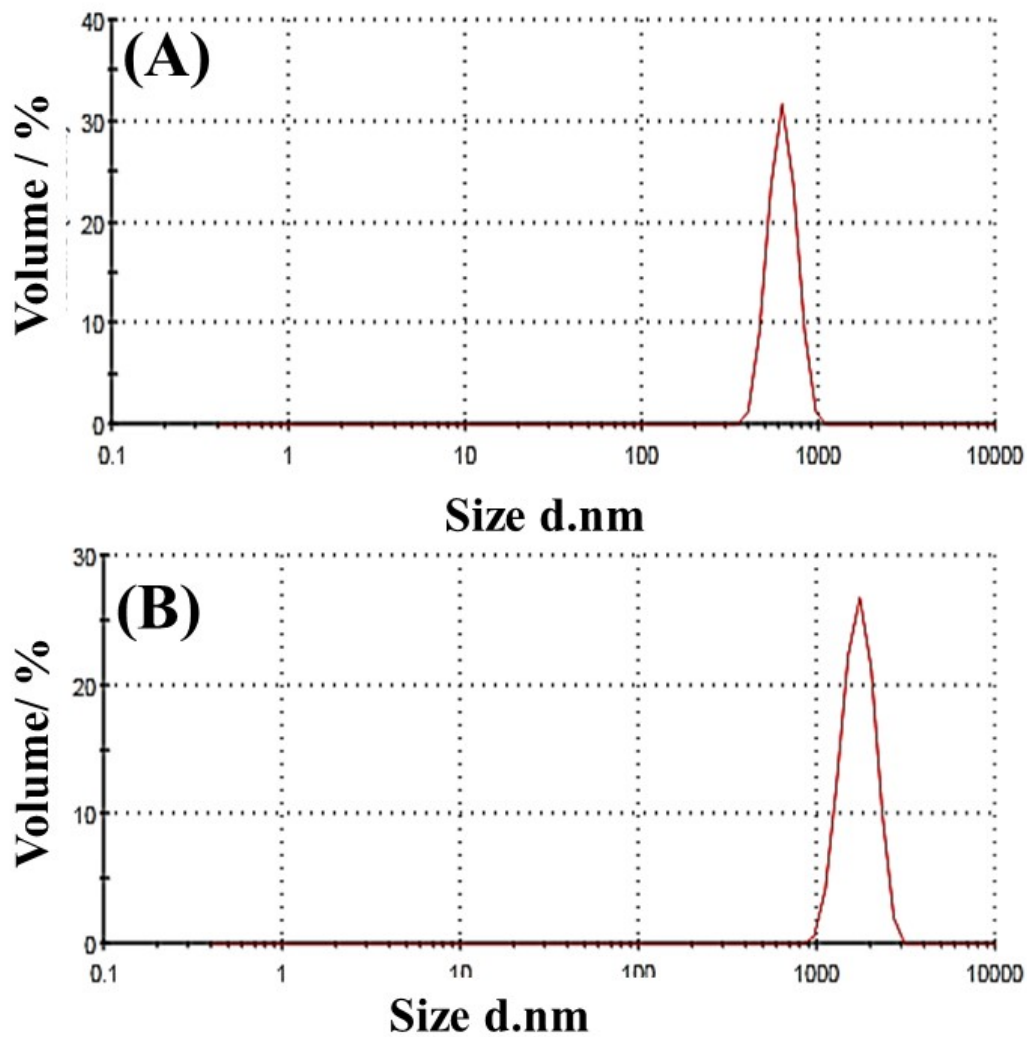


Figure. S<sub>5</sub>: Dynamic light scattering (DLS) measurement of (A) [ZM], and (B) [PZM].

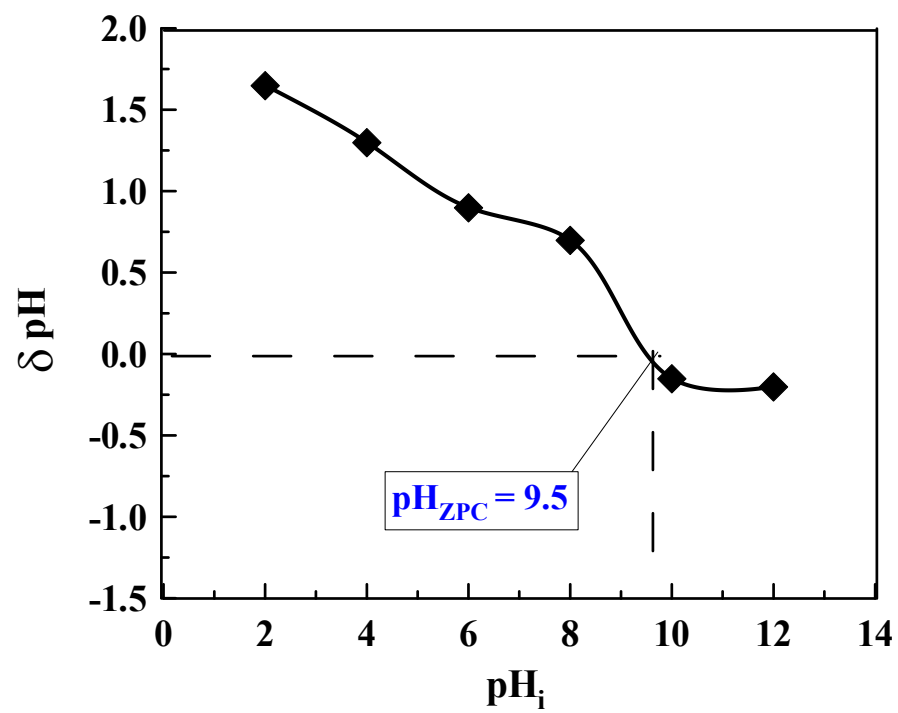
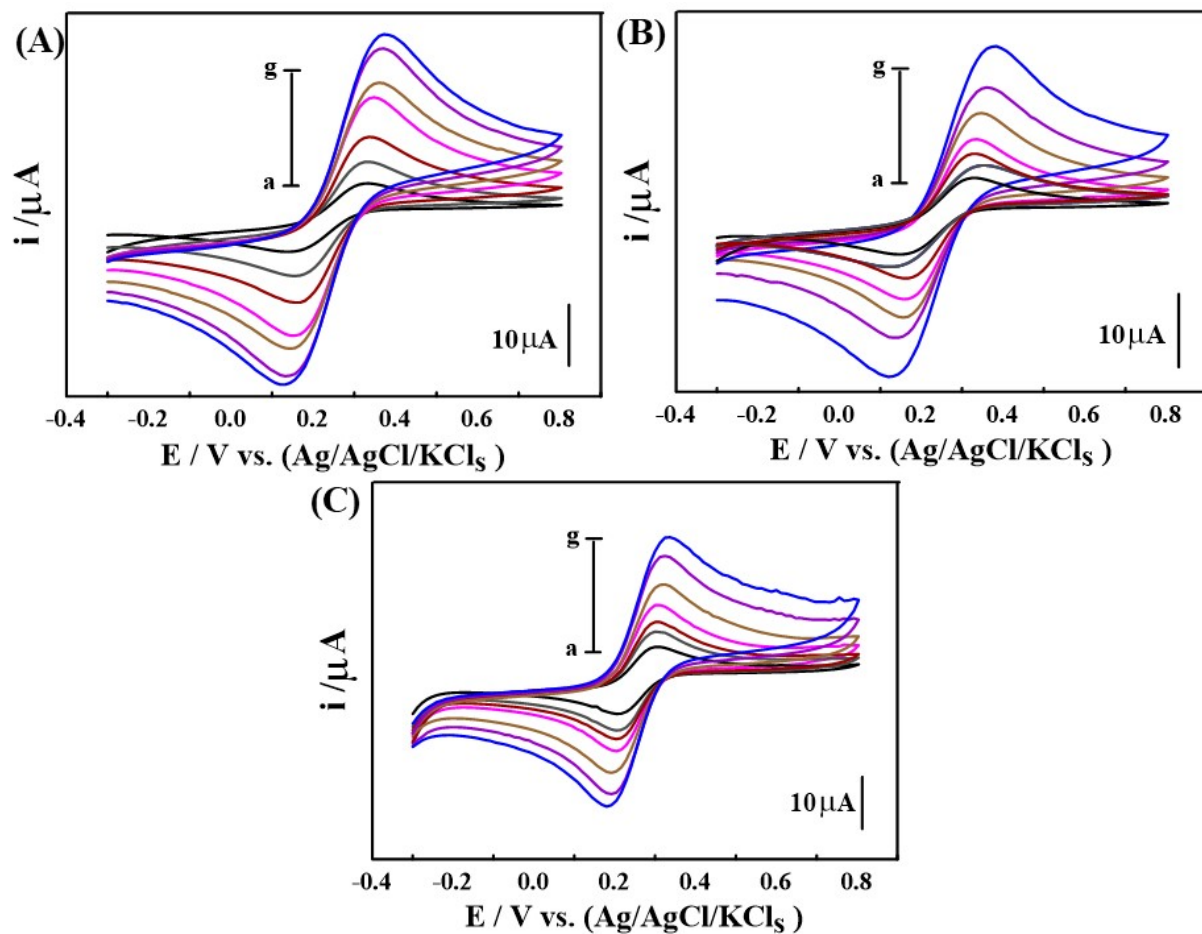
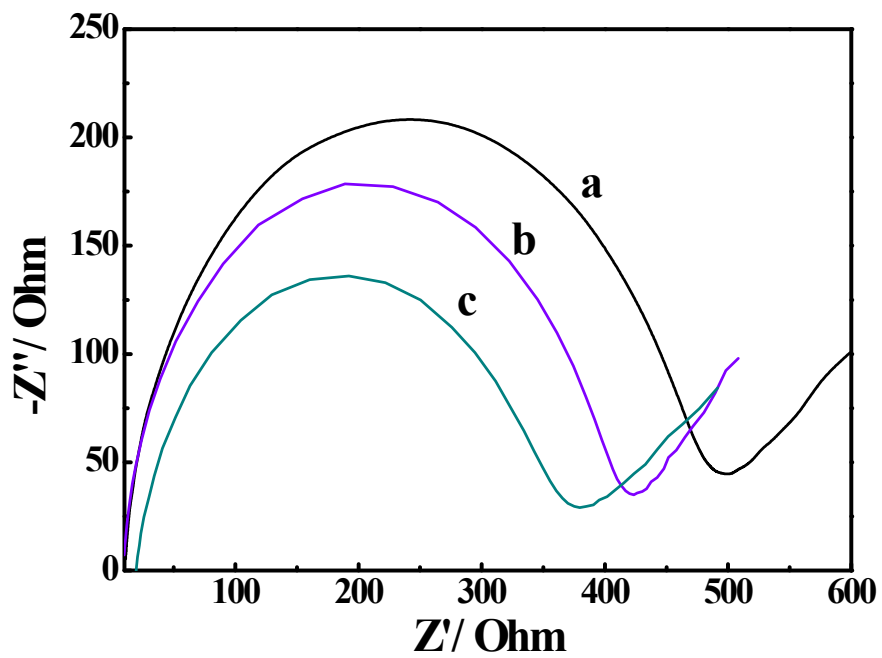


Figure. S<sub>6</sub>: The  $\text{pH}_{\text{ZPC}}$  value of [PZM].



**Figure. S7:** CVs of 5.0 mM  $K_3[Fe(CN)_6]$  in 0.1 M of KCl utilizing (A) BCPS, (B) [ZM], and (C) [PZM] MCPSs at different  $\nu \approx$  (a) 0.02, (b) 0.05, (c) 0.07, (d) 0.1, (e) 0.2, (f) 0.3, and (g) 0.4  $mV.s^{-1}$ .



**Figure.S8:** Nyquist plots of 5.0 mM of  $K_3[Fe(CN)_6]$  in 0.1 M of KCl utilizing (a) BCPS, (b) [ZM], and (c) [PZM] MCPSs.

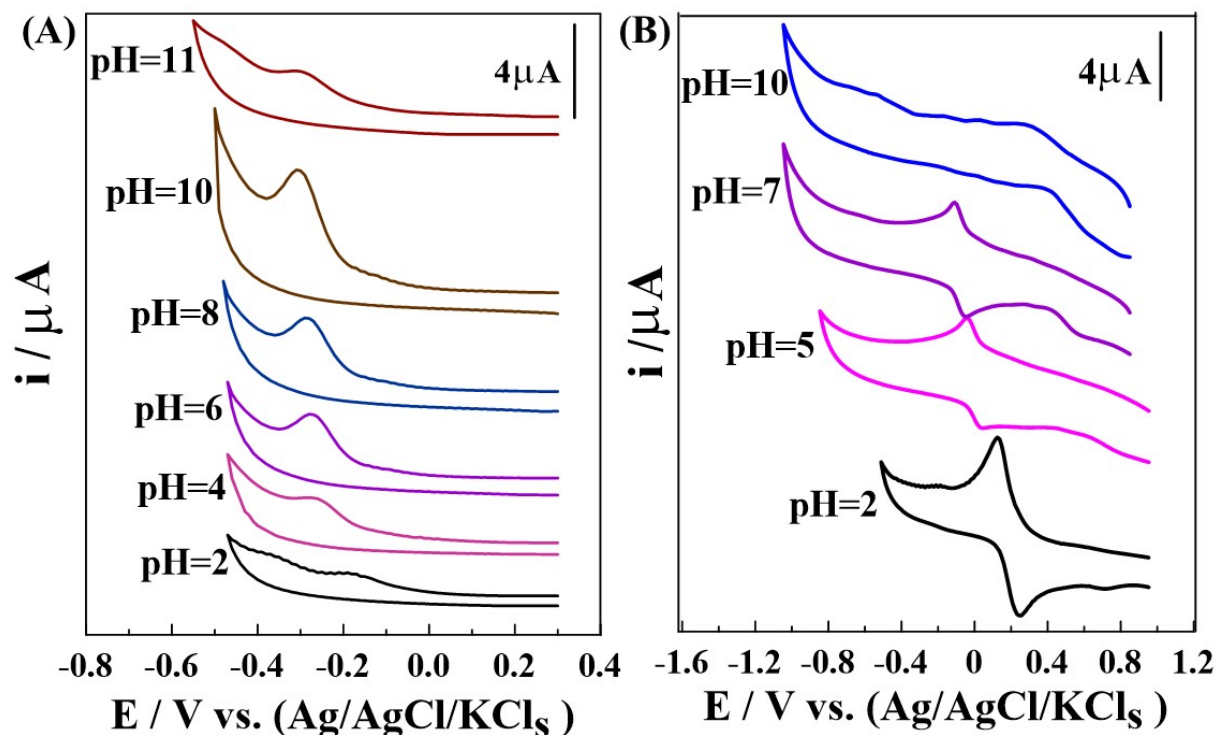


**Figure. S9:** CVs of (A) 0.1 nM of ART, and (B) 0.2 nM of DA were estimated using the [PZM] MCPS for a series of pH values with B–R universal buffer at  $\nu = 100 \text{ mV} \cdot \text{s}^{-1}$ .

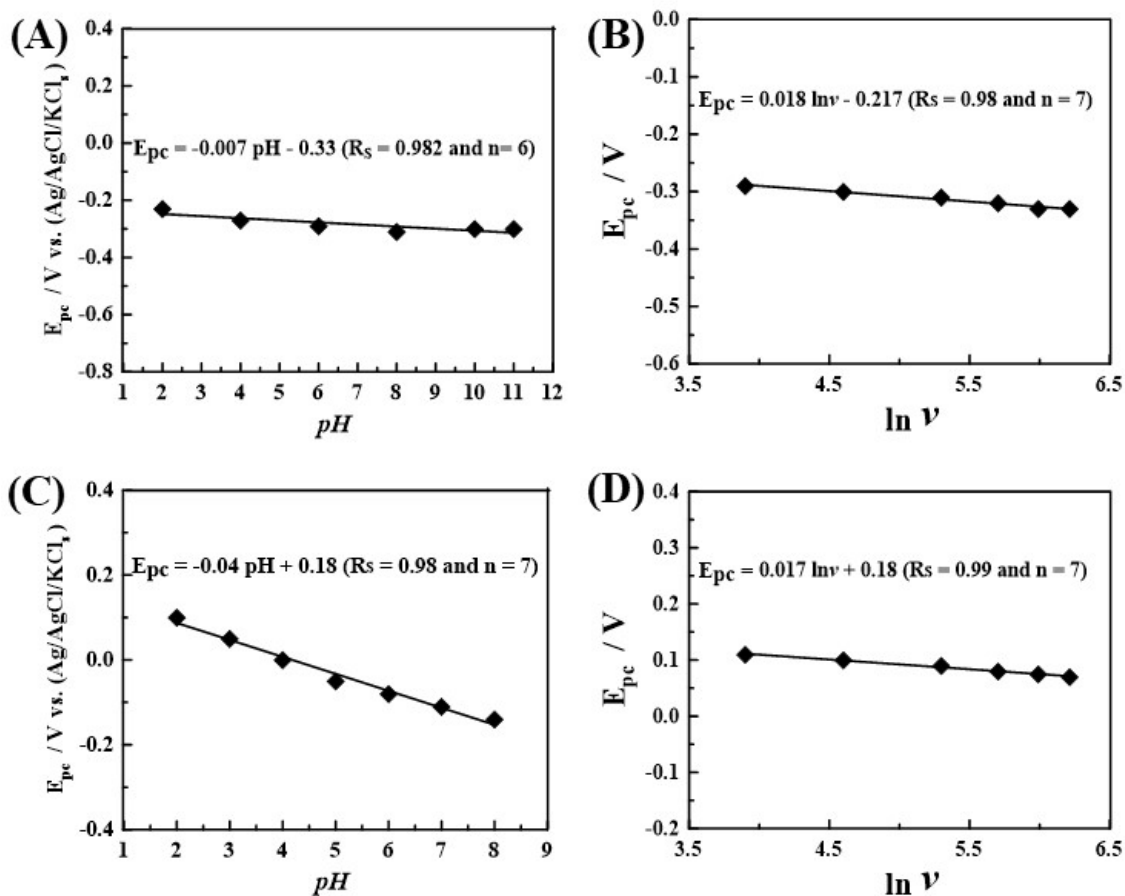


**Figure. S<sub>10</sub>:** Plots of (A)  $E_{pc}$  vs. pH, and (B)  $E_{pc}$  vs.  $\ln v$  of 0.1 nM ART (*pH 11*) at  $v = 100 \text{ mV}\cdot\text{s}^{-1}$  and  $v \approx 50 - 500 \text{ mV}\cdot\text{s}^{-1}$  ( $n = 3$ ), respectively. Plots of (C)  $E_{pc}$  vs. pH, and (D)  $E_{pc}$  vs.  $\ln v$  of 0.1 nM DA at  $v = 100 \text{ mV}\cdot\text{s}^{-1}$  and  $v \approx 50 - 500 \text{ mV}\cdot\text{s}^{-1}$  ( $n = 3$ ), respectively.

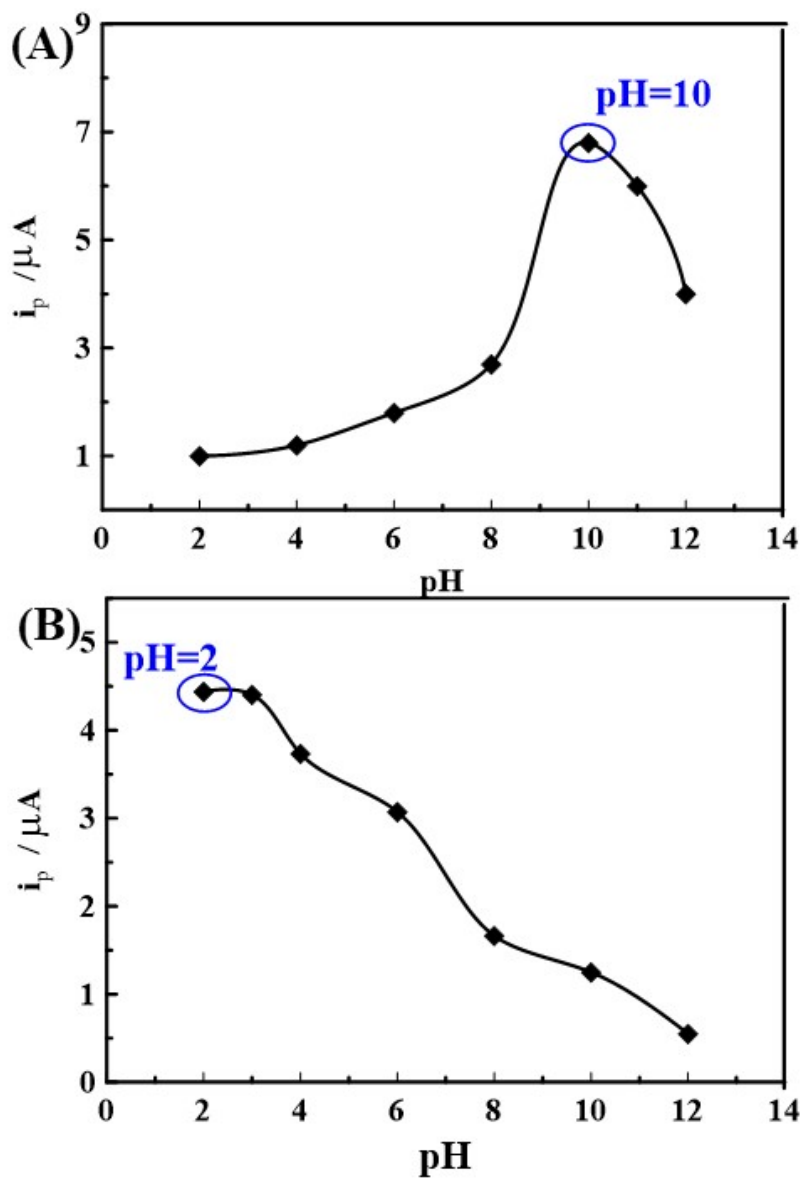


**Figure. S11:** The plot of the effect of different pH values (B–R universal buffer) of (A) 0.1 nM of ART at 0.3 V for 70s, and (B) 0.01 nM DA upon [PZM] MCPS by DP-AdCV at 0.7 V for 20s ( $f=120$  Hz,  $v=75$  mV, and  $a=40$  mV).

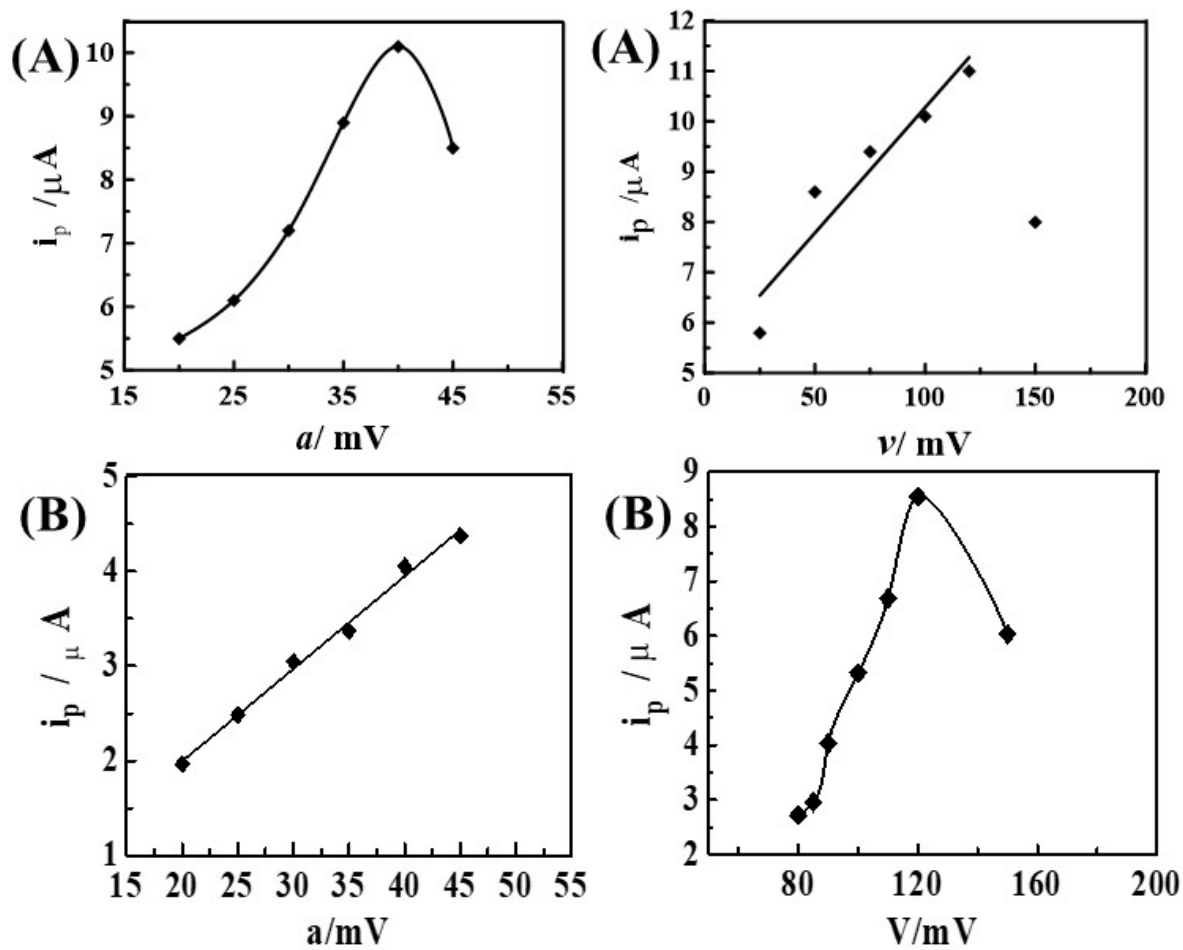


**Figure. S12:** Influence of pulse amplitude ( $a$ ), and scan rate ( $v$ ) parameters of (A) 0.1 nM of ART (pH 10), and (B) 0.01 nM DA (pH 2) upon [PZM] MCPS by DP-AdCV for 70s, respectively.



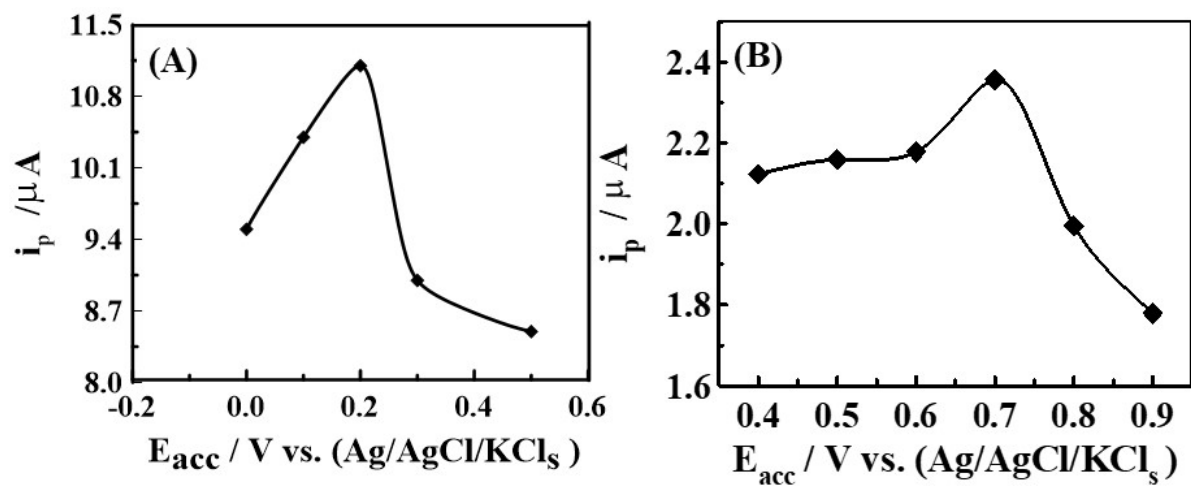


**Figure. S13:** (A) The effect of  $E_{\text{acc}}$  on the DP-AdCV signals of 0.1 nM of ART (pH 10) for 70s, and (B) 0.01 nM DA (pH 2) for 40s upon [PZM] MCPS by DP-AdCV ( $a= 45$  mV, and  $v=120$  mV).

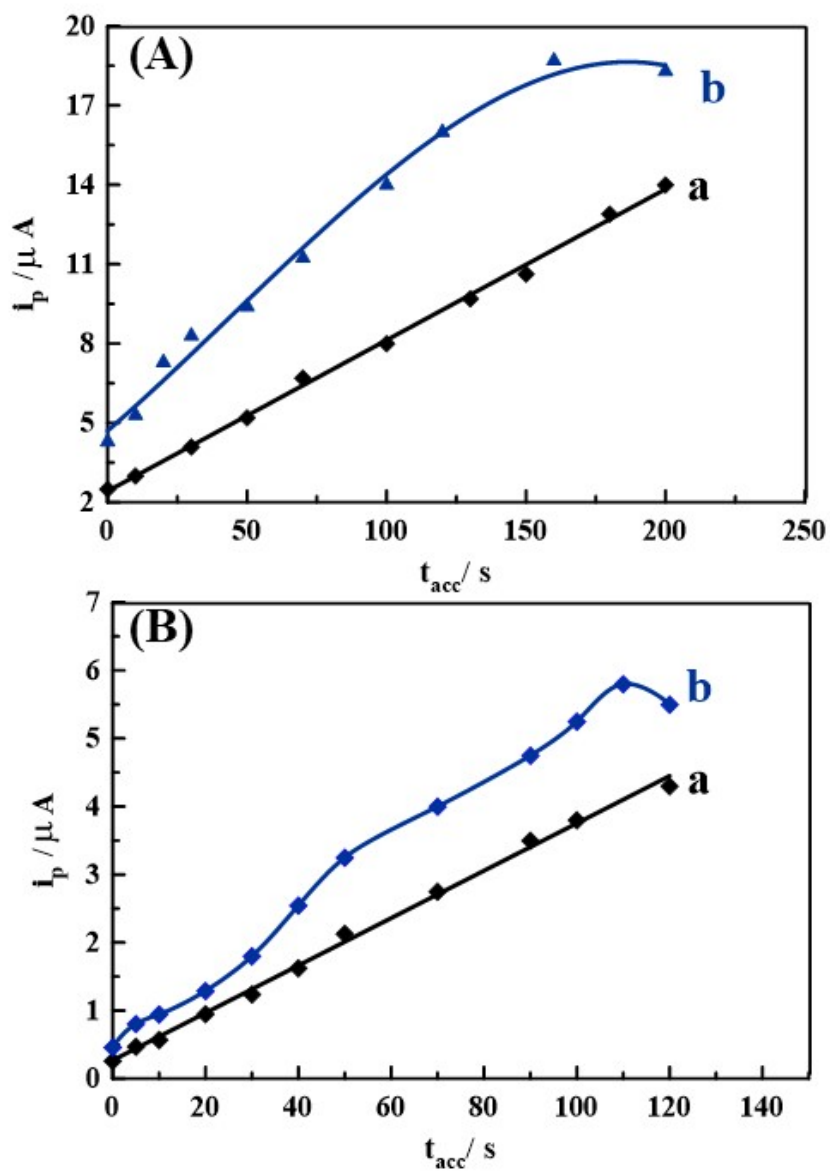


**Figure. S14:** The effect of  $t_{acc}$  on the DP-AdCV signals of (A) (a)5.0, and (b)10.0pM of ART (pH 10), and (B) (a)10.0, and (b) 15.0 pM of DA (pH 2) on [PZM] MCPS ( $v=120$  mV, and  $a= 45$  mV).

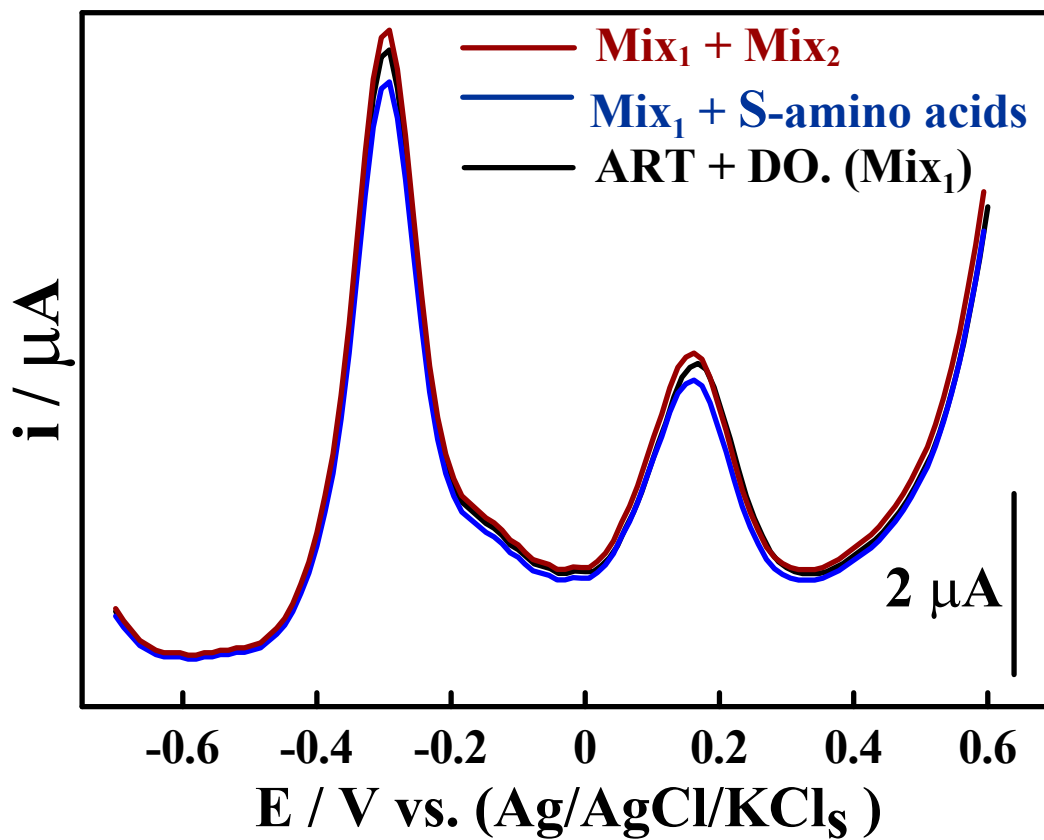


**Figure.S15:** DP-AdCV scans of 5.0 pM ART + 5.0 pM DA (**Mix<sub>1</sub>**) in the presence of 5.0 nM (~100-fold) of (**Mix<sub>2</sub>**; Cl<sup>-</sup>, CH<sub>3</sub>COO<sup>-</sup>, CO<sub>3</sub><sup>-2</sup>, BO<sub>3</sub><sup>-3</sup>, H<sub>2</sub>PO<sub>4</sub><sup>-</sup>, HPO<sub>4</sub><sup>-2</sup>, PO<sub>4</sub><sup>-3</sup>, and SO<sub>4</sub><sup>-2</sup>), and mixture of S-containing amino acids (cysteine (Cys) and thiamine (TA)).

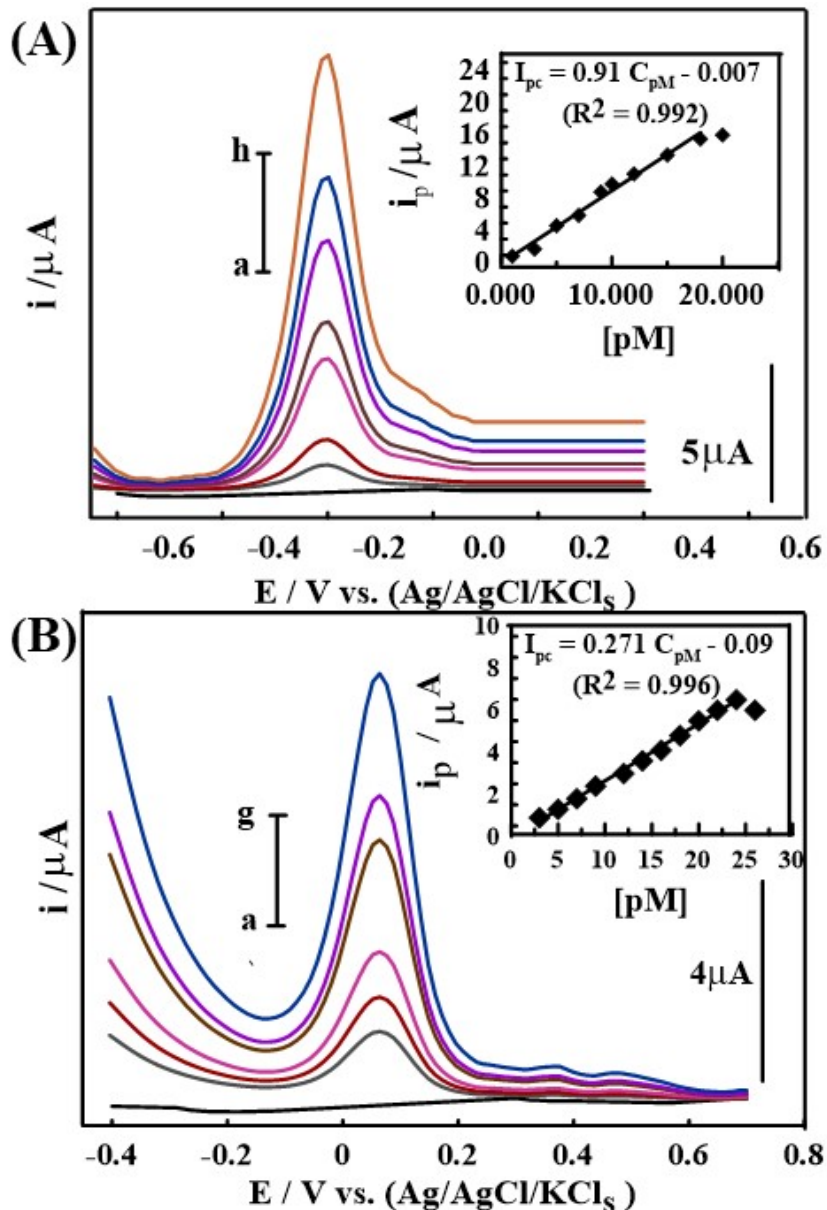


**Figure.S16:** DP-AdCV crests of different amounts of (A) ART in the B-R buffer (pH 10) on [PZM] MCPS at ( $a= 45$  mV, and  $v=120$  mV) for  $t_{acc}= 100$ s in human urine as follow: (a) Baseline, (b) 1.0, (c) 3.0, (d) 5.0, (e) 7.0, (f) 9.0, (g) 12.0, and (h) 18.0 pM. (B) DP-AdCV crests of different amounts of DA in the B-R buffer (pH 2) on [PZM] MCPS at ( $a= 45$  mV, and  $v=120$  mV) for 100s in human urine as follow: (a) Baseline, (b) 5.0, (c) 7.0, (d) 12.0, (e) 16.0, (f) 20.0, and (g) 24.0 pM at ( $a= 40$  mV, and  $v=120$  mV) for 100 s.

1. J. Rivera-Utrilla, I. Bautista-Toledo, M. A. Ferro-García and C. Moreno-Castilla, *Journal of Chemical Technology & Biotechnology*, 2001, **76**, 1209-1215.